AD-A232 637

NASA Contractor Report 187508
ICASE Report No. 91-9

ICASE

SECOND-ORDER CLOSURE MODELS FOR SUPERSONIC TURBULENT FLOWS

Charles G. Speziale
Sutanu Sarkar

DTIC
ELECTE
MAR 12 1991
S E D

Contract No. NAS1-18605
January 1991

Institute for Computer Applications in Science and Engineering
NASA Langley Research Center
Hampton, Virginia 23665-5225

Operated by the Universities Space Research Association

National Aeronautics and
Space Administration

Langley Research Center
Hampton, Virginia 23665

DISTRIBUTION STATEMENT A
Approved for public release;
Distribution Unlimited

Second-Order Closure Models for Supersonic Turbulent Flows

Charles G. Speziale and Sutanu Sarkar[1]

Institute for Computer Applications in Science and Engineering
NASA Langley Research Center
Hampton, VA 23665

ABSTRACT

Recent work by the authors and their colleagues on the development of a second-order closure model for high-speed compressible flows is reviewed. This turbulence closure is based on the solution of modeled transport equations for the Favre-averaged Reynolds stress tensor and the solenoidal part of the turbulent dissipation rate. A new model for the compressible dissipation is used along with traditional gradient transport models for the Reynolds heat flux and mass flux terms. Consistent with simple asymptotic analyses, the deviatoric part of the remaining higher-order correlations in the Reynolds stress transport equation are modeled by a variable density extension of the newest incompressible models. The resulting second-order closure model is tested in a variety of compressible turbulent flows which include the decay of isotropic turbulence, homogeneous shear flow, the supersonic mixing layer, and the supersonic flat-plate turbulent boundary layer. Comparisons between the model predictions and the results of physical and numerical experiments are quite encouraging.

Accession For
NTIS GRA&I ☒
DTIC TAB ☐
Unannounced ☐
Justification
By
Distribution/
Availability Codes
Dist | Avail and/or Special
A-1

QUALITY INSPECTED 3

[1]This research was supported by the National Aeronautics and Space Administration under NASA Contract No. NAS1-18605 while the authors were in residence at the Institute for Computer Applications in Science and Engineering (ICASE), NASA Langley Research Center, Hampton, VA 23665.

Report Documentation Page

1. Report No. NASA CR-187508 ICASE Report No. 91-9	2. Government Accession No.	3. Recipient's Catalog No.
4. Title and Subtitle SECOND-ORDER CLOSURE MODELS FOR SUPERSONIC TURBULENT FLOWS		5. Report Date January 1991
		6. Performing Organization Code
7. Author(s) Charles G. Speziale Sutanu Sarkar		8. Performing Organization Report No. 91-9
		10. Work Unit No. 505-90-52-01
9. Performing Organization Name and Address Institute for Computer Applications in Science and Engineering Mail Stop 132C, NASA Langley Research Center Hampton, VA 23665-5225		11. Contract or Grant No. NAS1-18605
		13. Type of Report and Period Covered Contractor Report
12. Sponsoring Agency Name and Address National Aeronautics and Space Administration Langley Research Center Hampton, VA 23665-5225		14. Sponsoring Agency Code

15. Supplementary Notes

Langley Technical Monitor: Michael F. Card

AIAA 29th Aerospace Sciences Meeting

Final Report

16. Abstract

Recent work by the authors and their colleagues on the development of a second-order closure model for high-speed compressible flows is reviewed. This turbulence closure is based on the solution of modeled transport equations for the Favre-averaged Reynolds stress tensor and the solenoidal part of the turbulent dissipation rate. A new model for the compressible dissipation is used along with traditional gradient transport models for the Reynolds heat flux and mass flux terms. Consistent with simple asymptotic analyses, the deviatoric part of the remaining higher-order correlations in the Reynolds stress transport equation are modeled by a variable density extension of the newest incompressible models. The resulting second-order closure model is tested in a variety of compressible turbulent flows which include the decay of isotropic turbulence, homogeneous shear flow, the supersonic mixing layer, and the supersonic flat-plate turbulent boundary layer. Comparisons between the model predictions and the results of physical and numerical experiments are quite encouraging.

17. Key Words (Suggested by Author(s)) compressible turbulence; second-order closure models; supersonic shear flows		18. Distribution Statement 34 - Fluid Mechanics and Heat Transfer Unclassified - Unlimited	
19. Security Classif. (of this report) Unclassified	20. Security Classif. (of this page) Unclassified	21. No. of pages 24	22. Price A03

NASA FORM 1626 OCT 86

NASA-Langley, 1991

1. Introduction

The ability to accurately predict high-speed compressible turbulent flows would have a variety of important technological applications in the design of advanced supersonic and hypersonic aircraft. Due to the wide range of scales exhibited in these flows, direct numerical simulations – with all scales resolved – are impossible for the foreseeable future. Furthermore, major operational problems with large-eddy simulations in complex wall-bounded geometries make their future application to these flows equally questionable. Consequently, the method of choice for the calculation of such complex aerodynamic flows continues to be based on Reynolds stress modeling and this is likely to remain true for the next several decades. Unfortunately, many of the improvements in the Reynolds stress modeling of incompressible turbulent flows that have been developed during the past two decades have not, for the most part, found their way into the calculation of the supersonic turbulent flows of aerodynamic importance. Design calculations still tend to be based on variable density extensions of simple eddy viscosity models such as that due to Baldwin and Lomax [1]. However, recent experience with incompressible turbulent flows indicate that significantly improved predictions can be obtained from more sophisticated two-equation models and second-order closures – particularly in flows with streamline curvature, a system rotation, and buoyancy or other body force effects (see Refs. [2 - 4]). While there have been some applications of second-order closure models to compressible turbulent flows [5 - 7], these studies did not make use of the newer incompressible models and did not explicitly account for dilatational effects in a physically consistent manner. This establishes the motivation for the present paper which is to provide a much more systematic approach to the development of compressible second-order closure models suitable for supersonic turbulent flows.

The compressible second-order closure model developed in this paper is based on the Favre-averaged Reynolds stress transport equation. It will be supplemented with a transport equation for the solenoidal part of the dissipation; the compressible dissipation is treated using the Sarkar, et al. [8] model which algebraically relates this term to the product of the solenoidal dissipation and the square of the turbulence Mach number. Gradient transport models are used for the Reynolds heat flux, mass flux, and turbulent transport terms along traditional lines. However, a new model for the pressure-strain correlation will be implemented based on the model developed recently by Speziale, Sarkar, and Gatski [9]. In addition, some of the newer developments in near wall turbulence modeling will be made use of [10]. An overview of the model's performance in a variety of test cases will be provided along with a brief discussion of needed future directions of research.

2. The General Model

Our analysis will be based on the governing equations of motion for an ideal gas which, neglecting body forces and bulk viscosity effects, are as follows:

Continuity

$$\frac{\partial \rho}{\partial t} + (\rho u_i)_{,i} = 0 \tag{1}$$

Momentum

$$\frac{\partial}{\partial t}(\rho u_i) + (\rho u_i u_j)_{,j} = -p_{,i} - \frac{2}{3}(\mu u_{j,j})_{,i} + [\mu(u_{i,j} + u_{j,i})]_{,j} \tag{2}$$

Energy

$$\frac{\partial}{\partial t}(\rho C_v T) + (\rho C_v u_i T)_{,i} = -p u_{i,i} + \Phi + (\kappa T_{,i})_{,i} \tag{3}$$

where

$$p = \rho R T \tag{4}$$

$$\Phi \equiv \sigma_{ij} u_{i,j} = -\frac{2}{3}\mu(u_{i,i})^2 + \mu(u_{i,j} + u_{j,i})u_{i,j} \tag{5}$$

given that ρ is the density, u_i is the velocity, p is the thermodynamic pressure, R is the ideal gas constant, μ is the dynamic viscosity, C_v is the specific heat at constant volume, T is the absolute temperature, σ_{ij} is the viscous stress tensor, Φ is the viscous dissipation, and κ is the thermal conductivity. In (1) - (5), the Einstein summation convention applies to repeated indices and $(\cdot)_{,i}$ denotes a gradient with respect to the spatial coordinate x_i. Any flow variable $\mathcal{F}$ can be decomposed into ensemble mean and fluctuating parts as follows:

$$\mathcal{F} = \overline{\mathcal{F}} + \mathcal{F}' \tag{6}$$

where, for a homogeneous turbulence, the mean $\overline{\mathcal{F}}$ can be taken to be a spatial average or, for a statistically steady turbulence, it can be taken to be a time average. An alternative decomposition based on mass weighted averages can be used wherein

$$\mathcal{F} = \tilde{\mathcal{F}} + \mathcal{F}'' \tag{7}$$

given that $\tilde{\mathcal{F}}$ is the Favre average which is defined as

$$\tilde{\mathcal{F}} = \frac{\overline{\rho \mathcal{F}}}{\overline{\rho}}. \tag{8}$$

As in the traditional studies of compressible Reynolds stress modeling, both (6) and (7) will be used.

A direct averaging of Eqs. (1) - (3) yields the mean continuity, momentum and energy equations which are as follows:

$$\frac{\partial \overline{\rho}}{\partial t} + (\overline{\rho}\tilde{u}_i)_{,i} = 0 \tag{9}$$

$$\frac{\partial}{\partial t}(\overline{\rho}\tilde{u}_i) + (\overline{\rho}\tilde{u}_i\tilde{u}_j)_{,j} = -\overline{p}_{,i} - \frac{2}{3}(\overline{\mu u_{j,j}})_{,i} + [\overline{\mu(u_{i,j} + u_{j,i})}]_{,j} - (\overline{\rho}\tau_{ij})_{,j} \tag{10}$$

$$\frac{\partial}{\partial t}(\overline{\rho}\overline{C}_v\tilde{T}) + (\overline{\rho}\tilde{u}_i\overline{C}_v\tilde{T})_{,i} = -\overline{p}\tilde{u}_{i,i} - \overline{p}\overline{u''_{i,i}} - \overline{p'u'_{i,i}} + \overline{\Phi} + (\overline{\kappa T_{,i}})_{,i} - Q_{i,i} \tag{11}$$

where $\overline{u''_i} \equiv \overline{-\rho' u'_i}/\overline{\rho}$ is the turbulent mass flux, $\overline{p'u'_{i,i}}$ is the pressure-dilatation correlation, and

$$\tau_{ij} = \widetilde{u''_i u''_j} \tag{12}$$

$$Q_i = \overline{\rho}\overline{C}_v \widetilde{u''_i T''} \tag{13}$$

are the Favre-averaged Reynolds stress tensor and Reynolds heat flux. Of course, $\overline{p} = \overline{\rho} R \tilde{T}$ is the mean pressure. The only assumption made in deriving (9) - (11) is that turbulent fluctuations in the specific heat C_v can be neglected.

For high-Reynolds-number turbulent flows, the molecular diffusion terms containing μ and κ are dominated by the turbulent transport terms except in a thin sublayer near the wall. If it is assumed that turbulent fluctuations in the viscosity, thermal conductivity and density can be neglected in this region, then the molecular diffusion terms can be approximated as follows:

$$\begin{aligned} \overline{\sigma}_{ij} &\equiv -\frac{2}{3}\overline{\mu u_{k,k}}\delta_{ij} + \overline{\mu(u_{i,j} + u_{j,i})} \\ &\approx -\frac{2}{3}\overline{\mu}\tilde{u}_{k,k}\delta_{ij} + \overline{\mu}(\tilde{u}_{i,j} + \tilde{u}_{j,i}) \end{aligned} \tag{14}$$

$$\overline{q}_i \equiv \overline{\kappa T_{,i}} \approx \overline{\kappa}\tilde{T}_{,i} \tag{15}$$

Eqs. (14) - (15) are made use of in virtually all of the existing compressible Reynolds stress models. The mean viscous dissipation $\overline{\Phi}$ can be decomposed as follows:

$$\begin{aligned} \overline{\Phi} &= \overline{\sigma}_{ij}\overline{u}_{i,j} + \overline{\sigma'_{ij}u'_{i,j}} \\ &= \overline{\sigma}_{ij}\tilde{u}_{i,j} + \overline{\sigma}_{ij}\overline{u''_{i,j}} + \overline{\rho}\epsilon \end{aligned} \tag{16}$$

where $\epsilon \equiv \overline{\sigma'_{ij}u'_{i,j}}/\overline{\rho}$ is the turbulent dissipation rate. Hence, in order to achieve closure, we need models for the following turbulence correlations:

(i) the Favre-averaged Reynolds stress τ_{ij}

(ii) the Favre-averaged Reynolds heat flux Q_i

(iii) the turbulent mass flux $\overline{u''_i}$

(iv) the turbulent dissipation rate ε

(v) the pressure-dilatation correlation $\overline{p'u'_{i,i}}$.

This is subject to the primary assumption that turbulent fluctuations in the viscosity, thermal conductivity, and specific heat can be neglected.

The Favre-averaged Reynolds stress tensor τ_{ij} is a solution of the transport equation

$$\begin{aligned} &\frac{\partial}{\partial t}(\overline{\rho}\tau_{ij}) + (\overline{\rho}\tilde{u}_k\tau_{ij})_{,k} = -\overline{\rho}\tau_{ik}\tilde{u}_{j,k} - \overline{\rho}\tau_{jk}\tilde{u}_{i,k} \\ &-C_{ijk,k} - \Pi_{ij} - \overline{\rho}\varepsilon_{ij} + \frac{2}{3}\overline{p'u'_{k,k}}\delta_{ij} - \overline{u''_i}\overline{p}_{,j} \\ &-\overline{u''_j}\overline{p}_{,i} + \overline{u''_i}\overline{\sigma}_{jk,k} + \overline{u''_j}\overline{\sigma}_{ik,k} + \overline{(u'_i\sigma'_{jk} + \overline{u'_j\sigma'_{ik}})}_{,k} \end{aligned} \tag{17}$$

where

$$C_{ijk} = \overline{\rho}\widetilde{u''_i u''_j u''_k} + \frac{2}{3}\overline{p'u'_k}\delta_{ij} \tag{18}$$

$$\Pi_{ij} = \overline{u_i' p'_{,j}} + \overline{u_j' p'_{,i}} - \frac{2}{3}\overline{u_k' p'_{,k}}\delta_{ij} \tag{19}$$

$$\varepsilon_{ij} = (\overline{\sigma_{ik}' u_{j,k}'} + \overline{\sigma_{jk}' u_{i,k}'})/\overline{\rho} \tag{20}$$

are the third-order diffusion correlation, the deviatoric part of the pressure-gradient velocity correlation, and the dissipation rate tensor. The viscous diffusion term is approximated by the relationship

$$\overline{u_i' \sigma_{jk}'} + \overline{u_j' \sigma_{ik}'} \approx \overline{\mu}(\tau_{ij,k} + \tau_{ik,j} + \tau_{jk,i}) \tag{21}$$

which is obtained by an asymptotic near wall analysis neglecting fluctuations in the viscosity as well as some higher-order correlations, particularly those involving dilatational effects. (In a high-Reynolds-number turbulent flow, the viscous diffusion effects would only be significant extremely close to the wall where the turbulence Mach number is small and, hence, Morkovin's hypothesis may be invoked.) The pressure-diffusion correlation $\overline{p' u_i'}$ can be written in terms of the Reynolds heat flux and mass flux as follows:

$$\overline{p' u_i'} = -\overline{\rho} R \tilde{T} \widetilde{u_i''} + \overline{\rho} R \widetilde{u_i'' T''}. \tag{22}$$

Gradient transport models are used for these quantities in the following form [11]

$$\widetilde{u_i''} = \frac{C_\mu}{\overline{\rho}\sigma_\rho}\frac{K^2}{\varepsilon}\overline{\rho}_{,i} \tag{23}$$

$$\widetilde{u_i'' T''} = -\frac{C_\mu}{\sigma_T}\frac{K^2}{\varepsilon}\tilde{T}_{,i} \tag{24}$$

where $K \equiv \frac{1}{2}\tau_{ii}$ is the turbulent kinetic energy and $C_\mu = 0.09$, $\sigma_T = 0.7$, and $\sigma_\rho = 0.5$ are dimensionless constants. The triple velocity correlation is modeled by using a traditional gradient transport hypothesis as follows [4]

$$\widetilde{u_i'' u_j'' u_k''} = -\frac{2}{3}C_s\frac{K^2}{\varepsilon}(\tau_{ij,k} + \tau_{ik,j} + \tau_{jk,i}) \tag{25}$$

where $C_s = 0.11$. Eq. (25) is the isotropized version of the gradient transport model introduced by Launder, Reece, and Rodi [12]. The advantage of this formulation lies in the fact that each turbulent transport term is coupled with a viscous term of the same form – a feature that arises from the isotropization of the model for the triple velocity correlation and the use of the true dissipation rather than the pseudo-dissipation in the formulation of the viscous terms in (21).

Now, we have to discuss the modeling of the remaining correlations needed for closure which consist of the deviatoric part of the pressure gradient-velocity correlation Π_{ij}, the pressure-dilatation correlation $\overline{p' u_{i,i}'}$, and the dissipation rate tensor ε_{ij}. Since our model is developed for high turbulence Reynolds numbers, the Kolmogorov assumption of isotropy of dissipation will be invoked sufficiently far from solid boundaries, i.e.,

$$\overline{\rho}\varepsilon_{ij} = \frac{2}{3}\overline{\rho}\varepsilon\delta_{ij} \tag{26}$$

where $\overline{\rho}\varepsilon = \overline{\sigma'_{ij}u'_{i,j}}$ is the scalar dissipation rate of the turbulence which appeared in Eq. (16). Following the work of Sarkar et al. [8], the dissipation rate will be decomposed into solenoidal and compressible parts as follows:

$$\varepsilon = \varepsilon_s + \varepsilon_c \tag{27}$$

where, for a homogeneous turbulence, $\overline{\rho}\varepsilon_s \equiv \overline{\mu\omega'_i\omega'_i}$ and $\overline{\rho}\varepsilon_c = \frac{4}{3}\overline{\mu(u'_{i,i})^2}$ given that ω'_i is the fluctuating vorticity. A comparable decomposition was recently introduced by Zeman [13] in an analysis of eddy shocklets. Based on a simple asymptotic analysis, a model for the compressible dissipation was derived by Sarkar et al. [8] wherein $\varepsilon_c = \alpha_1 M_t^2 \varepsilon_s$ given that $M_t = (2K/\gamma R\tilde{T})^{1/2}$ is the turbulence Mach number, $\gamma \equiv \overline{C}_p/\overline{C}_v$ is the ratio of specific heats, and α_1 is a dimensionless constant. A calibration based on direct numerical simulations of compressible isotropic turbulence yielded the final model [8]

$$\varepsilon = (1 + \alpha_1 M_t^2)\varepsilon_s \tag{28}$$

with $\alpha_1 = 1$. The asymptotic analysis that led to the development of (28) also indicated that the compressible dissipation is substantially larger than the pressure dilation correlation in compressible isotropic turbulence [8]. Consequently, at this stage of the modeling we neglect the pressure dilatation correlation, i.e., we set

$$\overline{p'u'_{i,i}} = 0. \tag{29}$$

Work is currently underway to develop more general models for the pressure-dilatation correlation suitable for high-speed flows with strong mean velocity gradients.

The *exact* transport equation for the solenoidal dissipation is of the general form

$$\frac{\partial(\overline{\rho}\varepsilon_s)}{\partial t} + (\overline{\rho}\tilde{u}_i\varepsilon_s)_{,i} = \mathcal{P}_{\varepsilon_s} - \Phi_{\varepsilon_s} + \mathcal{D}_{\varepsilon_s} - \frac{4}{3}\overline{\rho}\varepsilon_s\tilde{u}_{i,i} + (\overline{\mu}\varepsilon_{s,i})_{,i} \tag{30}$$

given that fluctuations in the viscosity can be neglected. Here, $\mathcal{P}_{\varepsilon_s}$ is the production of dissipation due to deviatoric strains, Φ_{ε_s} is the destruction of dissipation, and $\mathcal{D}_{\varepsilon_s}$ is the turbulent transport of dissipation (the precise form of the expressions for $\mathcal{P}_{\varepsilon_s}$, Φ_{ε_s} and $\mathcal{D}_{\varepsilon_s}$ are quite complicated and are omitted for simplicity). Consistent with the asymptotic analysis for the solenoidal dissipation, the higher-order correlations in (30) will be approximated by a variable density extension of the commonly used incompressible models. This yields a modeled transport equation for ε_s of the form

$$\begin{aligned}\frac{\partial(\overline{\rho}\varepsilon_s)}{\partial t} + (\overline{\rho}\tilde{u}_i\varepsilon_s)_{,i} = &-C_{\varepsilon 1}\overline{\rho}\frac{\varepsilon_s}{K}\tau_{ij}(\tilde{u}_{i,j} \\ &-\frac{1}{3}\tilde{u}_{k,k}\delta_{ij}) - \frac{4}{3}\overline{\rho}\varepsilon_s\tilde{u}_{i,i} - C_{\varepsilon 2}\overline{\rho}\frac{\varepsilon_s^2}{K} \\ &+(C_\varepsilon\overline{\rho}\frac{K}{\varepsilon_s}\tau_{ij}\varepsilon_{s,j})_{,i} + (\overline{\mu}\varepsilon_{s,i})_{,i}\end{aligned} \tag{31}$$

where $C_{\varepsilon 1} = 1.44$, $C_{\varepsilon 2} = 1.83$, and $C_\varepsilon = 0.15$ are dimensionless constants. In the incompressible limit, the standard form of the modeled dissipation rate equation is recovered [12].

It should be noted that, unlike in most previously proposed compressible models, mean dilatational effects are accounted for exactly by the second term on the r.h.s. of (31) – a feature that allows for the description of *compressed* isotropic turbulence as we will see later.

Finally, in order to close these equations, a model for the deviatoric part of the pressure gradient-velocity correlation Π_{ij} is needed. We will assume that, to the first-order, Π_{ij} can be approximated by a variable density extension of its incompressible form (i.e., the leading order effects of compressibility are through changes in the density). We will use a variable density extension of the SSG model which was recently derived by Speziale, Sarkar, and Gatski [9] for incompressible turbulent flows. This model takes the form:

$$\begin{aligned}\Pi_{ij} &= \overline{\rho}[(C_1\varepsilon + C_1^*\mathcal{P})b_{ij} - C_2\varepsilon(b_{ik}b_{kj} - \frac{1}{3}II\delta_{ij}) \\ &\quad -C_3K(b_{ik}\tilde{S}_{jk} + b_{jk}\tilde{S}_{ik} - \frac{2}{3}b_{mn}\tilde{S}_{mn}\delta_{ij}) \\ &\quad -C_4K(b_{ik}\tilde{W}_{jk} + b_{jk}\tilde{W}_{ik}) \\ &\quad -\frac{4}{5}K(1 - C^*II^{1/2})(\tilde{S}_{ij} - \frac{1}{3}\tilde{S}_{kk}\delta_{ij})]\end{aligned} \tag{32}$$

where

$$b_{ij} = \frac{(\tau_{ij} - \frac{2}{3}K\delta_{ij})}{2K} \tag{33}$$

$$\tilde{S}_{ij} = \frac{1}{2}(\tilde{u}_{i,j} + \tilde{u}_{j,i}), \quad \tilde{W}_{ij} = \frac{1}{2}(\tilde{u}_{i,j} - \tilde{u}_{j,i}) \tag{34}$$

$$\mathcal{P} = -\tau_{ij}\tilde{u}_{i,j}, \quad II = b_{ij}b_{ij} \tag{35}$$

and $C_1 = 3.4.$, $C_1^* = 1.80$, $C_2 = 4\ 2$, $C_3 = 1.25$, $C_4 = 0.40$, $C^* = 1.62$ are dimensionless constants. The SSG model was tested in a variety of incompressible, homogeneous turbulent flows where it was shown to yield improved predictions over older models such as the Launder, Reece, and Rodi model (see Speziale, Sarkar, and Gatski [9] for more details).

The complete form of our proposed compressible second-order closure model has now been provided for high turbulence Reynolds number flows. However, some discussion is needed concerning the integration of this model to a solid boundary. For attached boundary layers, wall functions can be used to bridge the outer and inner flows. If this is done, some of the newer wall functions that have been developed for supersonic turbulent boundary layers should be made use of (see He, Kazakia, and Walker [14] for an interesting discussion). On the other hand, with minor modifications, this second-order closure model can be integrated directly to a solid boundary – the preferred approach when there is separation or other complex alterations of the wall boundary conditions. In order to integrate the second-order closure model presented in this study to a solid boundary, two general alterations to the model are needed:

(a) the destruction of dissipation term in the modeled dissipation rate equation (31) must be damped to zero as the wall is approached. More precisely, $C_{\varepsilon 2}$ must be replaced by $C_{\varepsilon 2}f_2$ where $f_2 \to 1$ for $\mathrm{Re}_t \gg 1$ and $f_2 \to 0$ as $y \to 0$ (here, y is the coordinate normal to the wall and f_2 is $O(y^2)$ near the wall).

(b) A near wall correction to the deviatoric parts of the dissipation rate tensor and pressure gradient-velocity correlation must be provided.

Variable density extensions of existing incompressible models can be used as a first approximation (the reader is referred to Speziale, Abid, and Anderson [10], Launder and Shima [15], and Gatski et al. [16] for a more detailed discussion of near wall modeling). However, these near wall models involve wall damping functions that tend to be quite ad hoc. Consequently, a new approach is currently under development wherein only the momentum and turbulent kinetic energy equations are integrated to the wall; the individual components of the Reynolds stress tensor, as well as the dissipation rate equation, are only integrated to the edge of the viscous sublayer eliminating most of the need for wall damping.

Finally, it should be noted that for many practical applications to supersonic flows, it is more convenient to integrate the total energy equation for $E \equiv C_v T + \frac{1}{2}u_i u_i$ rather than the thermal energy equation (11). This equation takes the form

$$\begin{aligned}\frac{\partial}{\partial t}(\overline{\rho}\tilde{E}) + (\overline{\rho}\tilde{u}_i\tilde{E})_{,i} &= (\overline{\sigma}_{ij}\tilde{u}_j + \overline{\sigma}_{ij}\overline{u_j''} - \overline{p}\tilde{u}_i \\ &-\overline{p}\overline{u_i''} - \overline{q}_i)_{,i} + (\overline{\sigma'_{ij}u'_j} - \overline{p'u'_i} - \overline{\rho}\widetilde{E''u''_i})_{,i}\end{aligned} \tag{36}$$

where the energy flux is given by

$$\widetilde{E''u''_i} = \overline{C}_v\widetilde{T''u''_i} + \tau_{ij}\tilde{u}_j + \frac{1}{2}u''_i\widetilde{u''_j u''_j} \tag{37}$$

and the other correlations in (36) are modeled as previously described.

3. Applications of the Model

The first application to be considered is the decay of compressible isotropic turbulence with no mean dilatation (i.e., all components of $\tilde{u}_{i,j}$ are zero). In Figures 1(a) - (b), the results predicted by the model for the decay of the turbulent kinetic energy are compared with those obtained from direct numerical simulations (DNS) for initial turbulence Mach numbers $M_{t,0}$ of 0.1, 0.3, and 0.4 (these results are taken from Sarkar et al. [8]). It is clear that the model does an excellent job in reproducing the trends of the DNS which indicate a moderate *increase* in the decay rate of the turbulent kinetic energy with increasing turbulence Mach number. (The results should not be compared from a quantitative standpoint since the model is for high Reynolds number turbulence and the DNS is for $R_\lambda = 15$). This Mach number dependence of the turbulence decay rate is due to the compressible dissipation and cannot be described by the commonly used compressible turbulence models which neglect such dilatational effects. In Figure 2, the time evolution of the pressure-dilatation correlation obtained from the DNS of isotropic turbulence [8] is shown for an initial turbulence Mach number of $M_{t,0} = 0.5$. It is clear that after the early transient effects due to the initial conditions die out, the pressure-dilatation correlation becomes extremely small. This validates the assumption made of neglecting the pressure-dilatation to the lowest (isotropic) order.

The second problem that we will consider is the rapid compression or expansion of an isotropic turbulence. In this problem, a decaying isotropic turbulence is subjected to the mean dilatation

$$\tilde{u}_{i,j} = \begin{pmatrix} \frac{1}{3}\Gamma & 0 & 0 \\ 0 & \frac{1}{3}\Gamma & 0 \\ 0 & 0 & \frac{1}{3}\Gamma \end{pmatrix} \tag{38}$$

where Γ is a constant ($\Gamma > 0$ corresponds to an expansion whereas $\Gamma < 0$ represents a compression). We will consider rapid compressions and expansions for which $|\Gamma|K_0/\varepsilon_0 \gg 1$. The general model reduces to the following simple differential equations for this problem:

$$\dot{K} = -\frac{2}{3}\Gamma K - (1 + \alpha_1 M_t^2)\varepsilon_s \tag{39}$$

$$\dot{\varepsilon}_s = -\frac{4}{3}\Gamma\varepsilon_s - C_{\varepsilon 2}\frac{\varepsilon_s^2}{K}. \tag{40}$$

For $|\Gamma|K_0/\varepsilon_0 \gg 1$, the short-time solution to Eqs. (39) - (40) can be approximated as

$$K = K_0 \exp(-\frac{2}{3}\Gamma t) \tag{41}$$

$$\varepsilon_s = \varepsilon_{s,0} \exp(-\frac{4}{3}\Gamma t) \tag{42}$$

since the first term on the r.h.s. of (39) and (40) dominate. Hence, the integral length scale predicted by the model is as follows:

$$\Lambda = \Lambda_0 \exp\left(\frac{1}{3}\Gamma t\right) \tag{43}$$

since $\Lambda \propto K^{3/2}/\varepsilon_s$.

The results given in (41) and (43) are identical to those obtained by Reynolds [17] based on Rapid Distortion Theory (RDT). As correctly pointed out by Reynolds [17], many of the commonly used compressible turbulence models, unlike our model, erroneously predict that the integral length scale *decreases* with an expansion and *increases* with a compression. This problem arises from the neglect of the exact mean dilatational term $-\frac{4}{3}\overline{\rho}\varepsilon_s\tilde{u}_{i,i}$ that appears on the r.h.s. of (30).

Now, we will consider the problem of compressible, homogeneous shear flow. The model predictions will be compared with the direct numerical simulations conducted recently by Sarkar, Erlebacher, and Hussaini [18]. In this problem, an initially decaying compressible isotropic turbulence is subjected to a uniform shear S with the corresponding mean velocity gradients

$$\tilde{u}_{i,j} = \begin{pmatrix} 0 & S & 0 \\ 0 & 0 & 0 \\ 0 & 0 & 0 \end{pmatrix}. \tag{44}$$

In Figure 3, the time evolution of the turbulent kinetic energy predicted by our second-order closure model is compared with the predictions of the Launder, Reece, and Rodi (LRR) model and the results of direct numerical simulations [18] for the initial conditions

$SK_0/\varepsilon = 7.18$, $R_{\lambda_0} = 15$, and $M_{t_0} = 0.2$. It is clear from this figure that the new model does a better job in reproducing the trends of the simulations. (Some differences would be expected due to the fact that the model is for high turbulence Reynolds numbers whereas the simulations are for low R_λ). As discussed earlier, the compressible dissipation model (28) is based on the scaling

$$\frac{\varepsilon_c}{M_t^2 \varepsilon_s} = \text{constant}. \tag{45}$$

In Figure 4, the DNS results of Sarkar et al. [18] for the time evolution of $\varepsilon_c/M_t^2\varepsilon_s$ is shown for a variety of initial conditions. After the early time transient, $\varepsilon_c/M_t^2\varepsilon_s$ settles down to a constant value in the range of 0.5 to 0.6 thus validating the scaling assumed in (45). (We still leave $\alpha_1 = 1$ to account for the fact that we have neglected the pressure-dilatation correlation – a term which in shear flow has a comparable effect to the compressible dissipation.)

The next problem that we will consider is the plane supersonic mixing layer. In this problem, a supersonic stream mixes with a subsonic stream downstream of a splitter plate (see Figure 5). The calculations that we will present are an extension of those conducted by Sarkar and Balakrishnan [19] for a high-speed stream velocity $U_1 = 2500$ m/sec and a low-speed stream velocity $U_2 = 800$ m/sec. Both streams have the same thermodynamic quantities which are prescribed as follows: $T_1 = T_2 = 800°K$, $p_1 = p_2 = 1$ atm, and $\rho_1 = \rho_2 = 0.44$ kg/m^3. A convective Mach number M_c and spreading rate C_δ are defined by

$$M_c = \frac{U_1 - U_2}{a_1 + a_2} \tag{46}$$

$$\frac{d\delta}{dx} = C_\delta \left(\frac{U_1 - U_2}{U_1 + U_2}\right) \tag{47}$$

where δ is the thickness of the shear layer and a is the local speed of sound. In Figure 6, the normalized spreading rate $C_\delta/(C_\delta)_0$ obtained from our second-order closure model is compared with the experimental "Langley curve" for a variety of convective Mach numbers M_c. The comparison between the model predictions and experiments is quite good. In contrast to these results, a variable density extension of either the Launder, Reece, and Rodi model or the SSG model were *not* able to predict the dramatic drop in the spreading rate that occurs for convective Mach numbers $M_c > 1$ as shown in Figure 6. Consequently, it is clear that dilatational effects must be directly accounted for if supersonic shear layers are to be properly described. In Figures 7 - 8, the normalized streamwise turbulence intensity and turbulent shear stress predicted by the second-order closure model are compared with experimental data (here, $\Delta U = U_1 - U_2$). The predictions of the Launder, Reece, and Rodi model are also displayed. It is clear from these results that our model predictions are well within the range of the experimental data unlike those of the LRR model.

Finally, we will present some preliminary results for the supersonic flat plate turbulent boundary with an adiabatic wall and with wall cooling [20]. These calculations were done by a direct integration of this second-order closure model to the wall using damping functions as discussed at the end of Section 2. In Figure 9, the normalized skin friction predicted by the second-order closure model is compared with the Van Driest curve and experimental data for a range of external Mach numbers $0 \leq M_e \leq 10$ (the Reynolds number based on the momentum thickness $\mathrm{Re}_\theta = 10^4$). Clearly, the model predictions are in good agreement

with the experimental data. In Figure 10, the normalized skin friction predicted by this second-order closure model for the supersonic flat plate boundary layer with wall cooling is shown ($M_e = 4$, $\mathrm{Re}_\theta = 10^4$, T_w = wall temperature, and T_{aw} = adiabatic wall temperature). Again, the model predictions are in reasonably good agreement with the Van Driest curve. More detailed calculations of supersonic turbulent boundary layers are currently underway (Speziale and Abid [20]).

4. Concluding Remarks

A new and reasonably comprehensive second-order closure model has been developed for high-speed compressible turbulent flows. The features that distinguish this new model from previously proposed second-order closures for compressible turbulence lies in the explicit treatment of dilatational effects on the turbulence dissipation rate and the use of recently improved models for the pressure gradient-velocity and viscous diffusion correlations. Preliminary tests of the model in a variety of homogeneous and inhomogeneous supersonic turbulent flows were quite encouraging.

A substantial amount of research is still needed to refine the model. The major issues that need to be further explored are as follows:

(1) the development of an anisotropic correction to the model for the pressure-dilatation correlation valid for significant mean strain rates,

(2) the development of modeled transport equations for the Reynolds heat flux and mass flux terms that transcend the simple gradient transport models now being used, and

(3) the development of better near wall models that incorporate more compressible turbulence physics and are numerically robust.

In addition, the ability of this second-order closure model to predict the turbulence statistics in compressible flows with strong shocks remains to be demonstrated. Furthermore, if this model is to be extended to the hypersonic flow regime, real gas effects have to be incorporated into the model. All of these issues are currently under investigation in our ongoing research effort on compressible turbulence modeling.

Acknowledgements

The authors are indebted to Dr. T. B. Gatski for helpful discussions and Drs. R. Abid and L. Balakrishnan for their assistance in performing some of the computations presented in this paper.

References

[1] Baldwin, B. S. and Lomax, H., "Thin Layer Approximation and Algebraic Model for Separated Turbulent Flows," *AIAA Paper 78-257*, 1978.

[2] Lumley, J. L., "Computational Modeling of Turbulent Flows," *Adv. Appl. Mech.*, Vol. 18, pp. 123-176, 1978.

[3] Launder, B. E., "Phenomenological Modeling: Present and Future," *Proc. Whither Turbulence Workshop* (ed. J. L. Lumley), *Lecture Notes in Physics*, Vol. 357, pp. 439-485, Springer-Verlag, Berlin, 1990.

[4] Speziale, C. G., "Analytical Methods for the Development of Reynolds Stress Closures in Turbulence," *Ann. Rev. Fluid Mech.*, Vol. 23, pp. 107-157, 1991.

[5] Varma, A. K., Beddini, R. A., Sullivan, R. D., and Donaldson, C. duP., "Application of an Invariant Second-Order Closure Model to Compressible Turbulent Shear Layers," *AIAA Paper 74-592*, 1974.

[6] Vandromme, D., Minh, H. H., Viegas, J. R., Rubesin, M. W., and Kollmann, W., "Second-Order Closure for the Calculation of Compressible Wall Bounded Flows with an Implicit Navier-Stokes Solver," *Proceedings of the Fourth Symposium on Turbulent Shear Flows*, Karlsruhe, Germany, 1983.

[7] Haminh, H., Rubesin, M. W., Vandromme, D., and Viegas, J. R., "On the Use of Second-Order Closure Modelling for the Prediction of Turbulent Boundary Layer/Shock Wave Interactions: Physical and Numerical Aspects," *Proceedings of the International Symposium on Computational Fluid Dynamics*, Tokyo, Japan, 1985.

[8] Sarkar, S., Erlebacher, G., Hussaini, M. Y., and Kreiss, H. O., "The Analysis and Simulation of Compressible Turbulence," *J. Fluid Mech.*, in press.

[9] Speziale, C. G., Sarkar, S., and Gatski, T. B., "Modeling the Pressure-Strain Correlation of Turbulence – An Invariant Dynamical Systems Approach," *J. Fluid Mech.*, in press.

[10] Speziale, C. G., Abid, R., and Anderson, E. C., "A Critical Evaluation of Two-Equation Models for Near Wall Turbulence," *AIAA Paper* 90-1481, 1990.

[11] Cebeci, T. and Smith, A. M. O., *Analysis of Turbulent Boundary Layers*, Academic Press, New York, 1974.

[12] Launder, B. E., Reece, G. J., and Rodi, W., "Progress in the Development of a Reynolds Stress Turbulence Closure," *J. Fluid Mech.*, Vol. 68, pp. 537-566, 1975.

[13] Zeman, O., "Dilatation Dissipation: The Concept and Application in Modeling Compressible Mixing Layers," *Phys. Fluids A.*, Vol. 2, pp. 178-188, 1990.

[14] He, J., Kazakia, J. Y., and Walker, J. D. A., "Embedded Function Methods for Supersonic Turbulent Boundary Layers," *AIAA Paper 90-0306*, 1990.

[15] Launder, B. E. and Shima, N., "Second-Moment Closure for the Near Wall Sublayer: Development and Application," *AIAA J.*, Vol. 27, pp. 1319-1323, 1989.

[16] Gatski, T. B., Sarkar, S., Speziale, C. G., Balakrishnan, L., Abid, R., and Anderson, E. C., "Assessment and Application of Reynolds Stress Closure Models to High-Speed Compressible Flows," *AIAA Paper 90-5247*, 1990.

[17] Reynolds, W. C., "Fundamentals of Turbulence for Turbulence Modeling and Simulation," *Lecture Notes for Von Karman Institute, AGARD Lecture Series No. 86*, pp. 1-66, NATO, New York, 1987.

[18] Sarkar, S., Erlebacher, G., and Hussaini, M. Y., "Direct Simulation of Compressible Turbulence in Shear Flow," *Proceedings of the Lumley Symposium: Recent Developments in Turbulence*, ICASE, NASA Langley Research Center, 1990.

[19] Sarkar, S. and Balakrishnan, L., "Application of a Reynolds Stress Turbulence Model to the Compressible Shear Layer," *AIAA J.*, in press.

[20] Speziale, C. G. and Abid, R., "Second-Order Closure Modeling of Near Wall Turbulent Flows," in preparation.

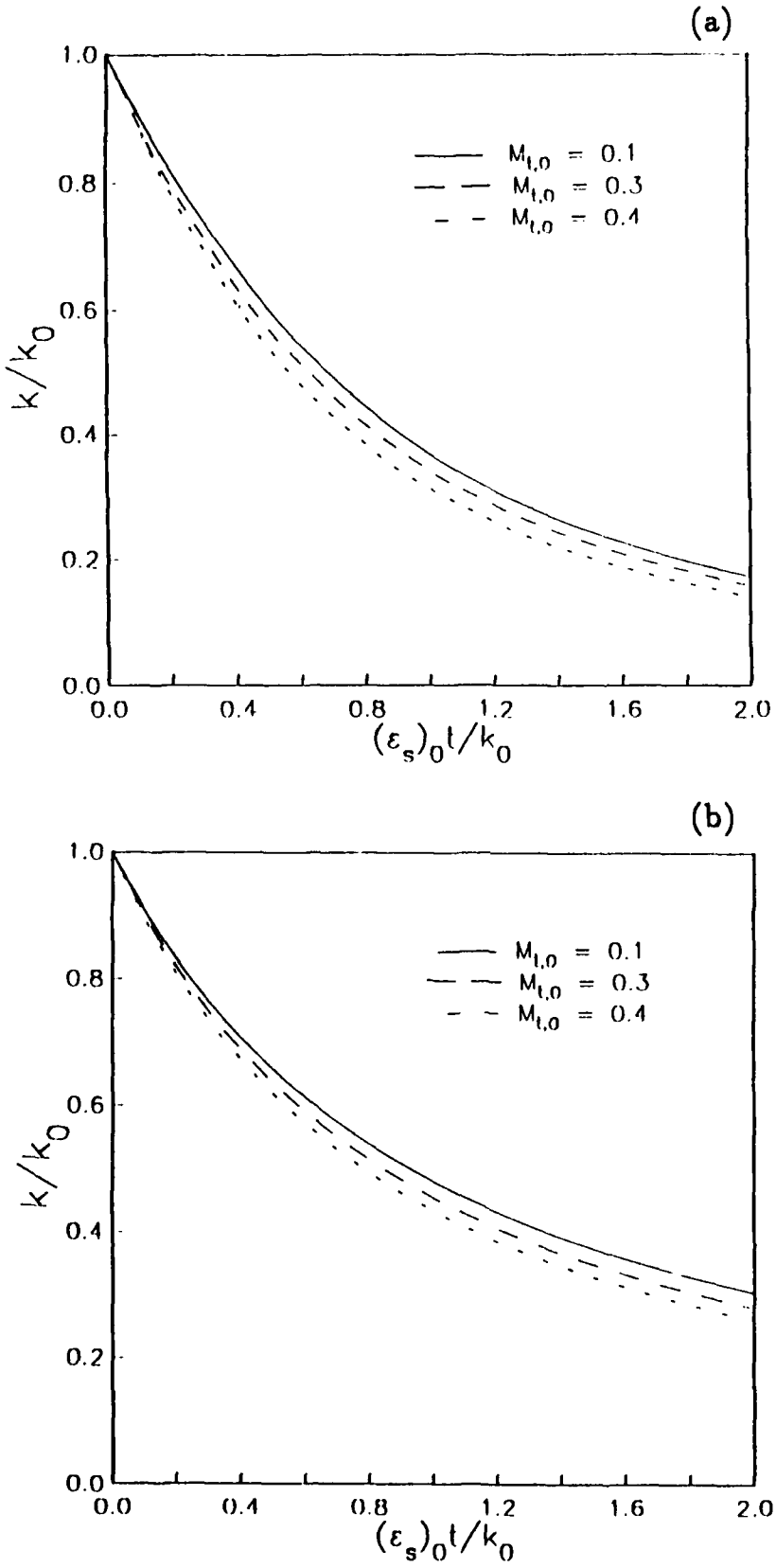

Figure 1. The decay of turbulent kinetic energy in compressible isotropic turbulence for initial turbulence Mach numbers $M_{t,0} = 0.1$, 0.3, and 0.4. (a) Direct Numerical Simulations [8], (b) Model Predictions.

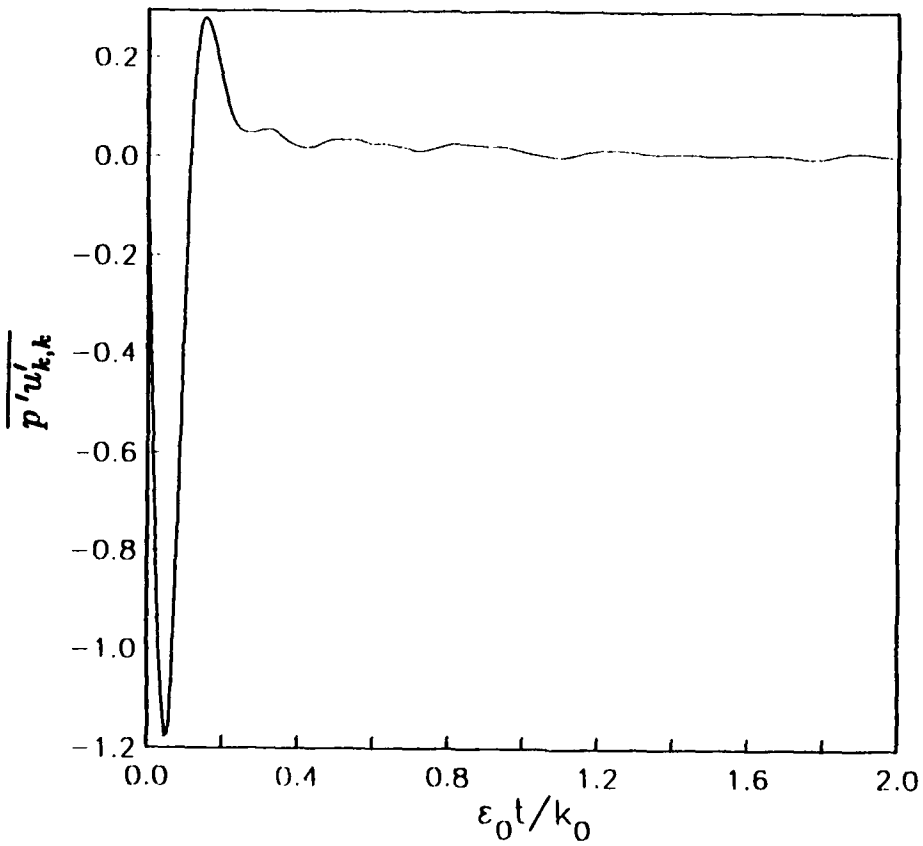

Figure 2. Time evolution of the pressure-dilatation correlation in compressible isotropic turbulence obtained from Direct Numerical Simulations [8] ($R_{\lambda_0} = 15$, $M_{t_0} = 0.5$).

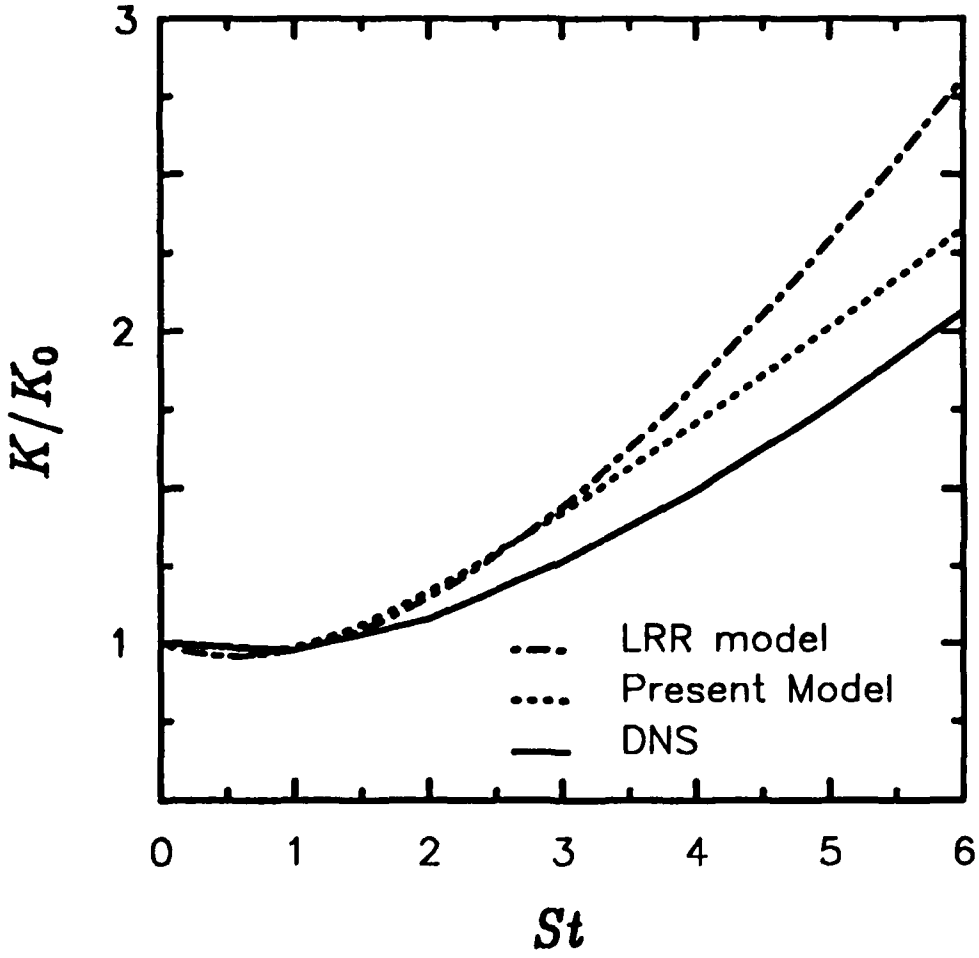

Figure 3. Time evolution of the turbulent kinetic energy in homogeneous shear flow ($R_{\lambda_0} = 15$, $M_{t_0} = 0.2$, $SK_0/\varepsilon_0 = 7.18$): —— Direct Numerical Simulations [18]; – · – LRR Model; · · · Current Model.

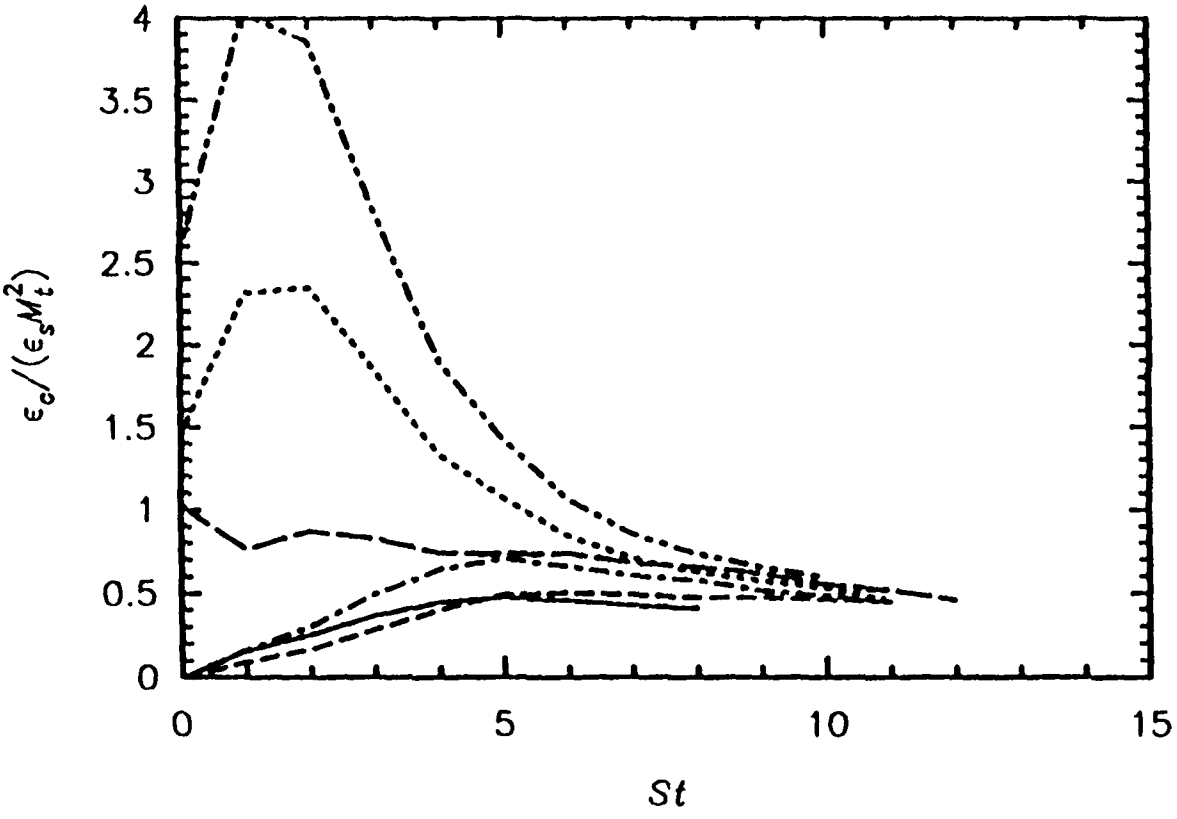

Figure 4. Time evolution of $\varepsilon_c/M_t^2\varepsilon_s$ in homogeneous shear flow obtained from Direct Numerical Simulations [18] for a variety of initial conditions (the initial turbulence Mach number M_{t_0} varies from 0.2 to 0.5).

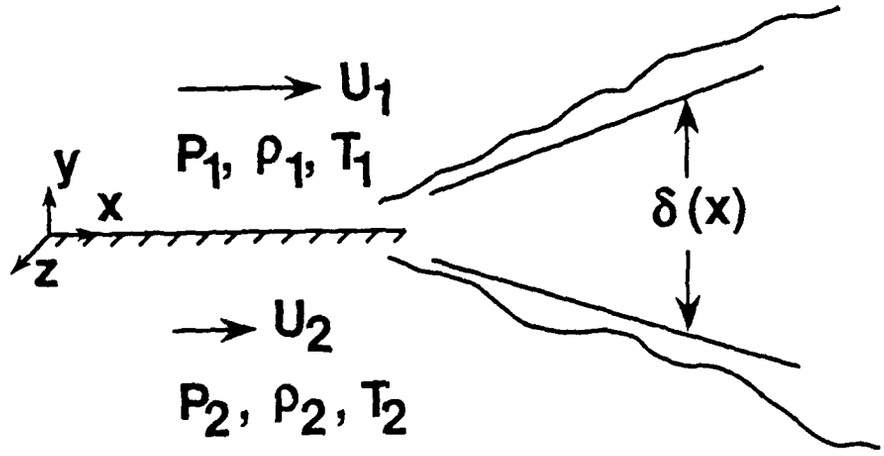

$$M_c = \frac{U_1 - U_2}{a_1 + a_2}$$

$$\frac{d\delta}{dx} = C_\delta \left(\frac{U_1 - U_2}{U_1 + U_2}\right)$$

Figure 5. Schematic diagram of the supersonic mixing layer.

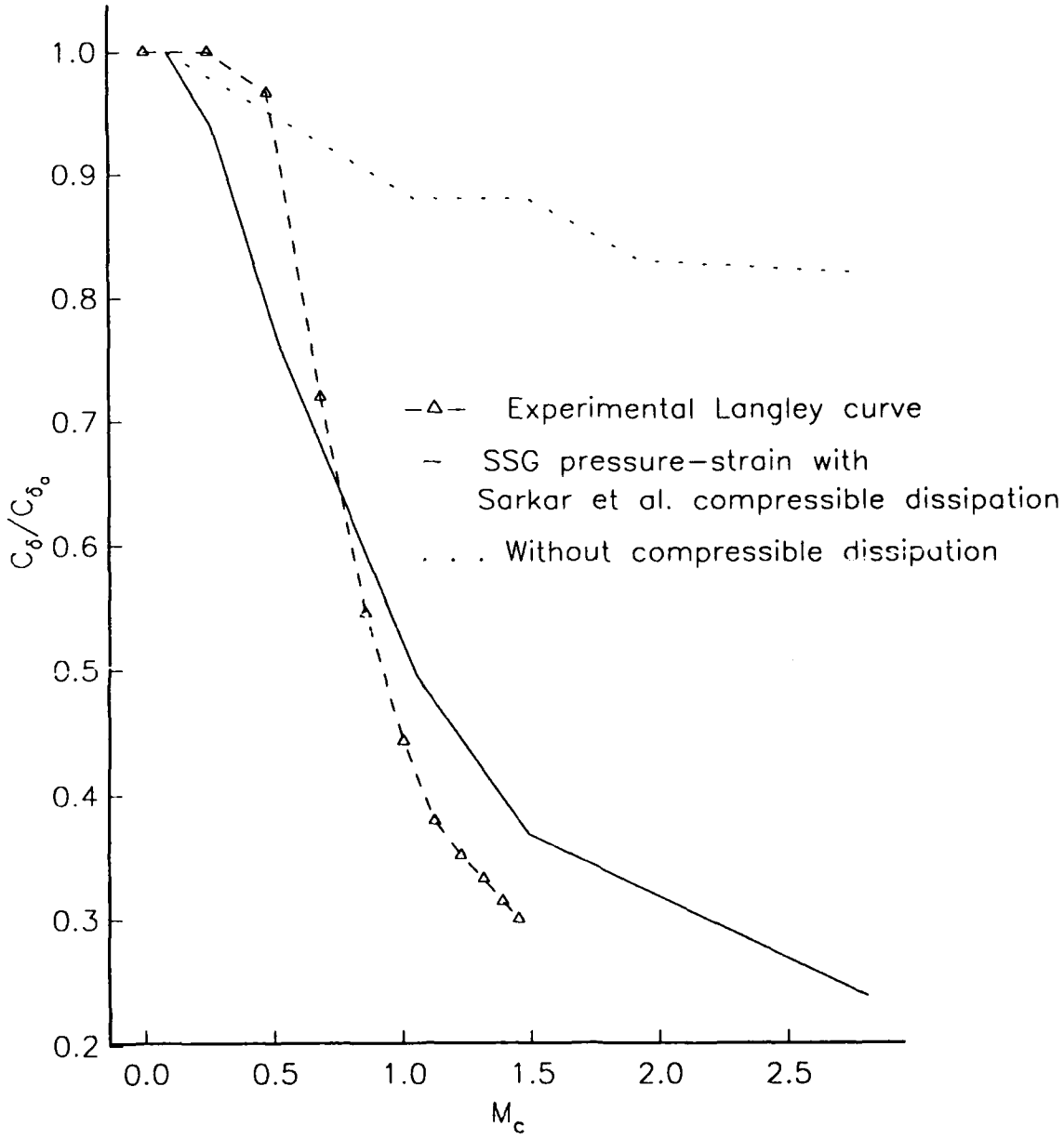

Figure 6. Normalized spreading rate as a function of the convective Mach number M_c: comparison of the model predictions with experimental data for the supersonic mixing layer. —— Current Model; ···· LRR Model; △ Experimental "Langley Curve" (Refs. [16,19]).

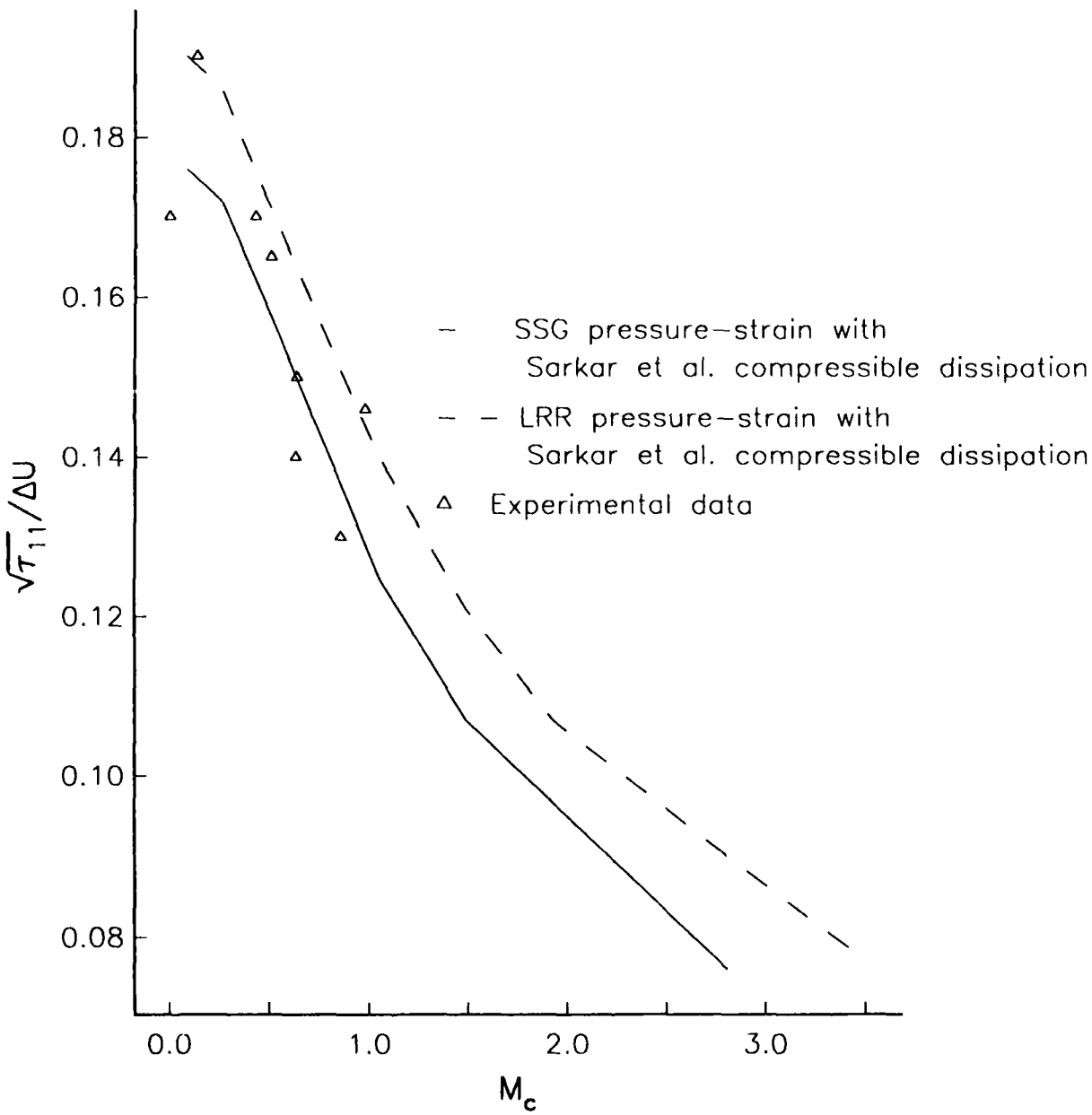

Figure 7. Normalized maximum streamwise turbulence intensity as a function of the convective Mach number. —— Current Model; - - - LRR Model; ∧ Experimental Data (Refs. [16,19]).

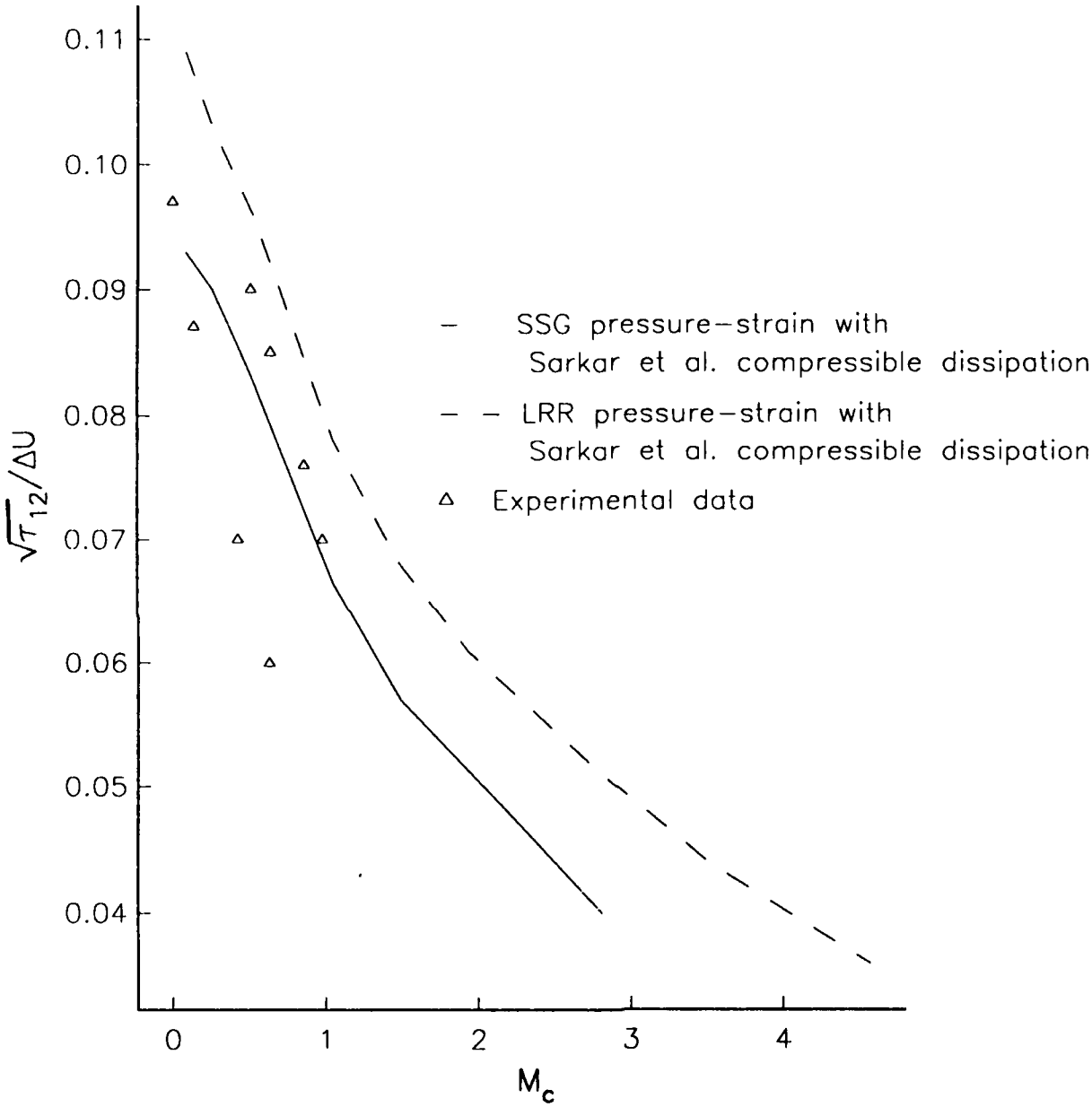

Figure 8. Normalized maximum turbulent shear stress as a function of the convective Mach number. —— Current Model; – – – LRR Model; △ Experimental Data (Refs. [16,19]).

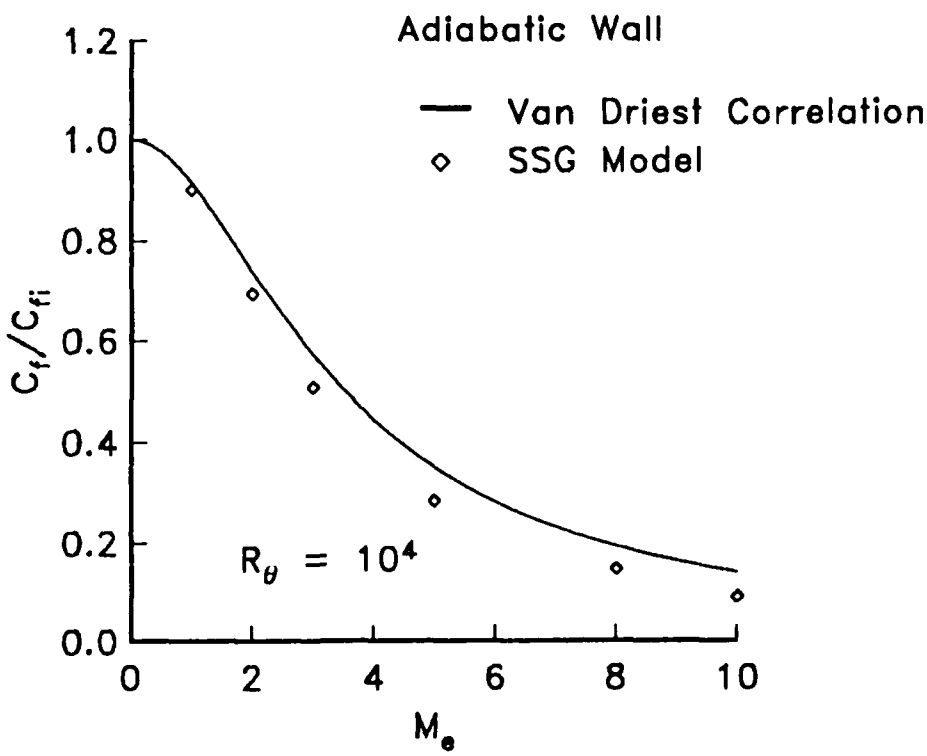

Figure 9. Normalized skin friction as a function of the external Mach number M_e for the compressible flat plate turbulent boundary layer with an adiabatic wall ($\mathrm{Re}_\theta = 10^4$): ◇ Model Predictions; —— Van Driest Curve.

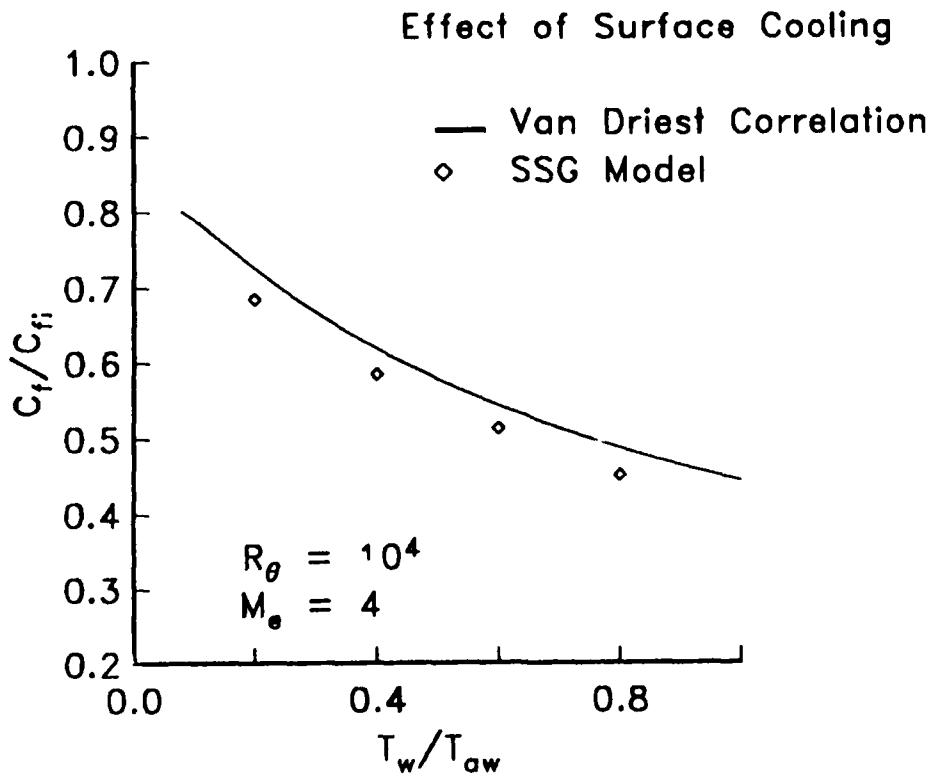

Figure 10. Normalized skin friction as a function of wall temperature T_w/T_{aw}: the effect of surface cooling on the compressible flat plate turbulent boundary layer for an external Mach number $M_e = 4$ ($\mathrm{Re}_\theta = 10^4$). ◇ Model Predictions; —— Van Driest Curve.